Acta of Bioengineering and Biomechanics
Vol. 16, No. 3, 2014

Original paper
DOI: 10.5277/abb140303

Three dimensional finite element analysis of a novel osteointegrated dental implant designed to reduce stress peak of cortical bone

LI ZHENG[1,2], JINGSONG YANG[2], XUEFENG HU[2], JIAOMING LUO[3]*

[1] The Medical and Scientific Research Center of Guangxi Medical University, Guangxi Medical University, Nanning, Guangxi, China.
[2] Research Center of Regenerative Medicine of Guangxi Medical University, Nanning, Guangxi, China.
[3] National Engineering Research Center for Biomaterials, Sichuan University, Chengdu, Sichuan, China.

A new type of dental implant was designed as multi-component mainly including inset and abutment between which a gap was introduced to guide the force to transmit from the cancellous bone to cortical bone, with the intention to lower the stress peak at cortical bone. By way of finite element analysis (FEA) associated with advanced computer tomography (CT) and 3D model reconstruction technology to construct precise mandible model, biomechanical aspects of implant were investigated. Compared with traditional implant that created stress dominantly at cortical bone, stress peak at the implant/bone interface in the cervical cortex decreased sharply (about 51%) for the new type of implant. Furthermore, applying varying implant shape and gap dimensions helped to optimize the design of this new implant. Optimization results revealed that: (1) screwed cylindrical implant is superior to tapered, stepped and smooth cylindrical implant in effectively decreasing the stress peak of bone; (2) deepening and widening gap would contribute to the decline of stress peak, but at the cost of break and destruction of the inset; (3) suitable gap size with the depth of 7 mm and width of 0.3 mm would be applicable. This work may provide reference for clinical application of dental implant.

Key words: *FEA, CT, dental implant, design, cervical cortex, stress distribution*

1. Introduction

In terms of the Mechanostat concept, bone is maintained if the forces acting on it are in an equilibrium state [1], [2]. Inadequate stresses cause disuse atrophy of the bone, while excessive local stresses around an implant result in pressure necrosis of the host bone, microfractures and marginal bone loss with potential implant failure [3], [4]. From biomechanical view, rational stress distribution obtained in bone surrounding dental implants is critical to maintain the bone–implant interface and determine the success of dental implants [4], [5].

To investigate stress distribution at the bone/implant interface, finite element analysis (FEA) is a useful tool that has been applied to dental systems to simulate behavior under masticatory loading. The stress distribution around dental implants has been studied by FEA, indicating that the main stress peaks arise around the neck of the implant in the upper cortical layer [6]–[8]. The risk of implant failure due to excessive stress concentration in marginal bone has often been recognized. Some studies have emphasized the importance of implant designs which can reduce the level of stress at the neck of the implant [9]–[12]. And it was shown that stresses in cancellous bone were considerably lower than those in cortical bone [13]. It was hypothesized that designs intended for transmitting stress from cancellous bone to cortical bone may be effective in reducing stress peaks of cortical bone.

* Corresponding author: Jiaoming Luo, National Engineering Research Center for Biomaterials of Sichuan University at Wangjiang Road 29# in Chengdu of China. Tel: +86-02885410563, Fax: +86-02885412848, e-mail: jmluo@scu.edu.cn
Received: September 10th, 2013
Accepted for publication: January 7th, 2014

But the obstacle is how to design the implant that can effectively transfer stress to cortical bone via cancellous bone.

In this paper, a new type of dental implant with the intention to create stress initially at cancellous bone to reduce the stress peaks in the surrounding upper cortical bone was designed and evaluated by FEA. The analysis was carried out based on improved accuracy of mandible model by introducing computer tomography (CT) technology [14], [15], with precise definition of both the geometry and the mechanical properties, which was closer to the real condition. Furthermore, implant shape and parameters were studied to predict the dimensional effects on stress distribution of bone, in order to optimize the implant design. This work was intended to lend references for clinical application of dental implant.

2. Materials and methods

2.1. The design of the new type of dental implant

The new type of dental implant consisted of three parts: an inset, an abutment and an airtight circle. The whole system was an axisymmetrical cylindrical solid, with its symmetrical profile shown in Fig. 1. The abutment was implanted into the jaw bone, with the inset secured to the abutment by screw connection at the region of segment B and segment C. Different from the typical design of dental implant, a gap with certain depth and length between the inset and abutment was introduced, intended to transfer forces from cancellous bone to cortical bone instead of the traditional way of transmitting forces directly to surrounding cortical layer. For the inset, the depth of the gap, i.e., the length of segment A below the circle, can be adjusted by altering the length of segment C. The joint area of segments B and C in touch with the abutment was designed to be slope with edge filleted to buffer the force transmitted to this area. The airtight circle, made of Telfon, was added at the outlet to serve the role of sealing.

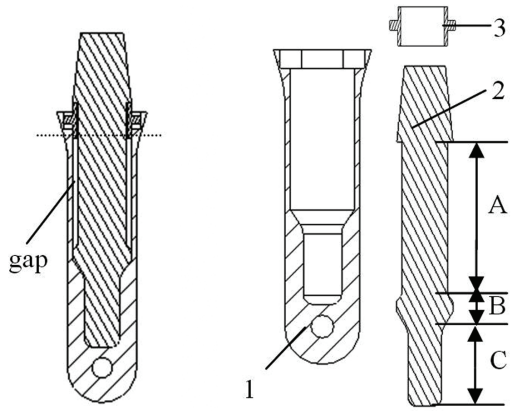

Fig. 1. Design of the new type of dental implant
(left: the assembly; right: the disassembled component:
1 – abutment; 2 – inset; 3 – airtight circle)

2.2. The construction of the three dimensional FE model

2.2.1. CAD model of mandible

The geometry and material data were acquired from CT slices of the mandible of a 25-year-old female. Figure 2a shows typical sections within the whole sections. The maximum available spatial resolution within a slice is about 0.5 mm and about 1 mm between two slices. The CT value for the cortical bone is from 1200 to 2012 HU, averaged about 1600 HU, while for the cancellous bone ranged from 500 to 900 HU. Each pixel possesses an information depth of 16 Bit (65536 grey values). Resolutions of the 2D-Slices are 512 × 512.The data are given in the DICOM format and can be read into the CAD software. Outer shape of the mandible in each slice can be easily obtained, for

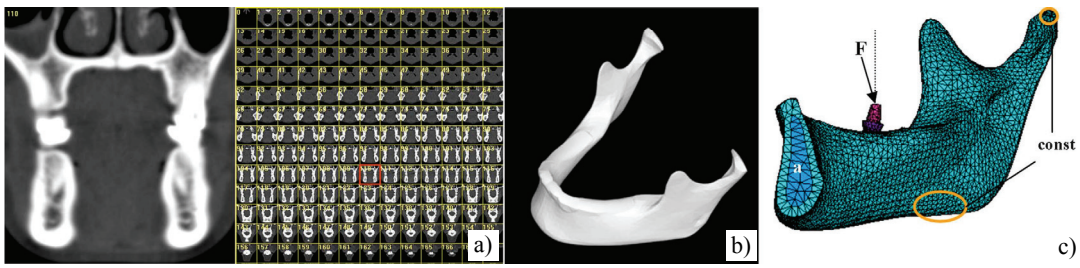

Fig. 2. Construction of FE model of mandible with implant:
(a) CT sections of human mandible, (b) CAD model of mandible, (c) FE model of mandicle

the density in the grey values differs significantly from the surrounding tissue. But the border between the cortical plate and the cancellous inner region is hard to be reliably detected; only an approximate borderline was drawn. After 2D-segmentation was done by selecting and modifying the contours, 3D CAD model of mandible with cortical and cancellous zones was reconstructed (Fig. 2b).

2.2.2 Building FE model of mandible bone with new type of implant

The following were measured from the CT data: the height of cortical bone is about 28–30 mm, the distance of buccal-lingual side is about 13–15 mm, and a 2~3 mm thick cortical bone surrounded the cancellous bone at the upper side.

The new type of dental implant was implanted in the second premolar position, with implant diameter of 4 mm and thread length of 14 mm in the bone. The depth and the width of the gap were 7 mm and 0.3 mm, respectively. Having trivial effect on the analysis result, the circle was omitted for analysis. As for the symmetry of mandible, only a half was adopted. Besides, the crown was out of calculation for economic reasons. The assembling of the bone and implant was accomplished in CAD environment. Meanwhile, traditional cylindrical implant that was only one-part was selected as control group.

2.2.3. Material properties for the FE models

After being converted to FE model using the software of ANSYS 10.0 (ANSYS Inc., Southpointe, PA), mechanical properties were assigned to the components as follows: the dental implant was made of titanium alloy (TC4) with elastic modulus of 116 GPa and Poisson' s ratio of 0.3; the cortical bone was with a constant elastic modulus of 15 GPa and Poisson's ratio of 0.3; the cancellous bone was classified as dense, with elastic modulus of 1.5 GPa and Poisson's ratio of 0.3. Both the implant and the bone were assumed to be isotropic, homogeneous, and linear elastic.

2.2.4. Constraints and load cases

Simulating the static state after the period of osseointegration, the implant was assumed to be integrated to the cortical bone and cancellous bone. For the new type of implant, the interface of the inset part and the abutment was defined as fully binded. There is no relative movement assumed within the integrated parts which allows them to share the same nodes. Element type of eight-noded solid 185 was chosen to free mesh the assembly, with contact region refined. As a result, 112174 and 111577 nodes were created for the new type of implant and traditional one, respectively. In agreement with the anatomic studies, all degrees of freedom of the nodes at the mandible bottom and the condyles (marked in Fig. 2c), the attachment regions of the masticatory muscles to prevent the rotation of the model around the condyles, were constrained, as shown in Fig. 2c. Symmetrical boundary condition was applied to the symmetrical surface of bone (a in Fig. 2c). On the buccal cusps of the fixed prostheses, 400 N 15°oblique forces [16] (F in Fig. 2c), simulating biting force in adults at premolars, [17] were applied. FEA analysis was carried out using ANSYS software.

2.2.5. Optimization of the new type of implant

Dimensional effects of the implant parameters on stress distribution of bone for the new type of implants, focusing on the depth and width of the gap, were predicted. The geometrical dimensions are listed in Table 1.

Implant shape effects was another factor to be investigated. In this study, smooth cylindrical, stepped, tapered and screw-surfaced cylindrical implants were selected for the abutment part of the new type of implant. Furthermore, as for screw implant, the full length and pitch size of screw as the influencing factors were studied. In Table 2, the main dimensions of four screw implant models are listed.

For all the implants, the same loading and boundary conditions were applied.

Table 1. Main dimensions of the implant model

	Implant symbol						
	d-0 mm	d-2 mm	d-3 mm	d-5 mm	d-7 mm	d-9 mm	w-0.5 mm
Gap depth (mm)		2	3	5	7	9	9
Gap width (mm)		0.3	0.3	0.3	0.3	0.3	0.5

Table 2. Dimensions of screw implant

	Implant number			
	(s1)	(s2)	(s3)	(s4)
Pitch size (mm)	7	7	10	10
Screw length (mm)	0.7	0.4	0.7	0.4

3. Results

The results were displayed as 2D contour plots or path plots of von Mises stress.

3.1. Comparison of the new type of implant with the traditional one

2D contour plots of von Mises stress of mandible with implant for the new type of implant and traditional one are shown in Fig. 3a, c, respectively. Also, corresponding contour plots of components where the stress peak (MX) of the whole system occurred were given (Fig. 3b, d). From the results, it was shown that the stress peak (MX) was located at the dental implant at the lingual side for both types. The difference is the region of implant and the value. For the new type of implant, the value of stressstress peak positioned at the bottom area of segment A of the inset amounted to 674 MPa. For traditional implant, the value of it was just at the exit of the contacting area with the upper cortical layer that has the maximal stress of 150 MPa.

Figure 4a, b shows the stress distribution at the interface of bone with hidden implant from cutaway view. Maximal stress (MX) was at the border of cortical bone and cancellous bone for the new implant, and at the topside of the interfacial upper cortical layer for traditional implant, both at the lingual side. For comparison, maximal stress of bone declined from 98.9 MPa of traditional implant system to 47.9 MPa of the new implant system, almost 51.6%.

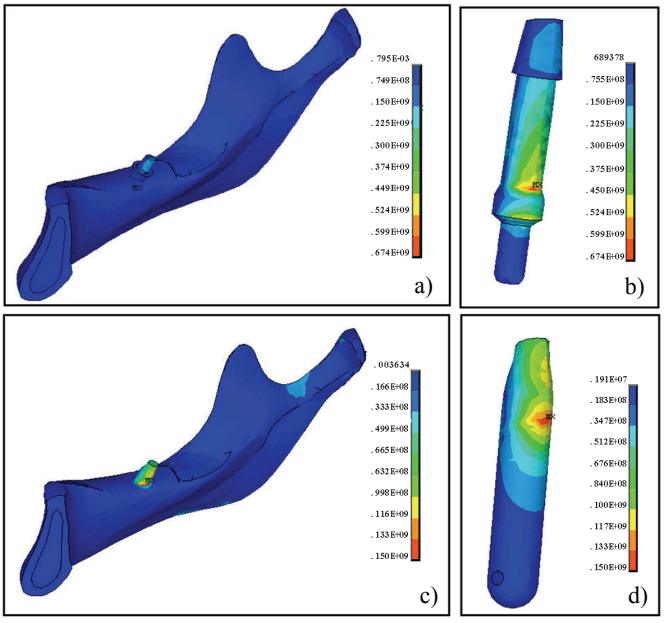

Fig. 3. Contour plots of Von Mises stress distribution of implants and bone:
(a, b – new implant with gap depth of 7 mm and width of 0.3 mm; c, d – traditional implant)

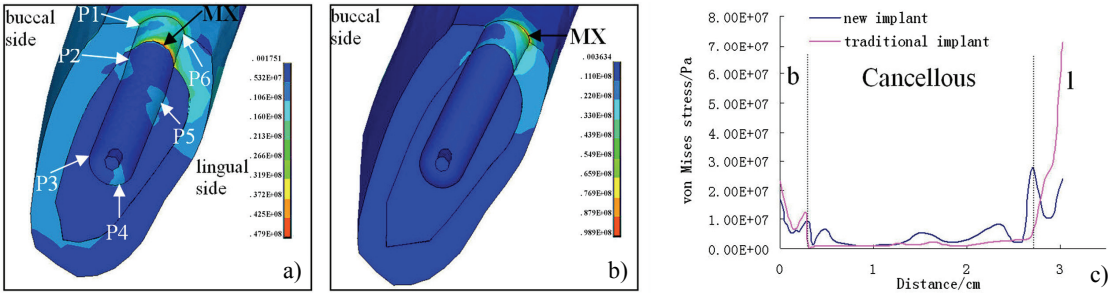

Fig. 4. Contour plots and path plots of von Mises stress distribution of bone:
a, b – contour plots of stress distribution of bone; c – path plots of interfacial stress distribution along P1-P2-P3-P4-P5-P6 (a)

Path plots of von Mises stress distribution of bone at the implant/bone interface along P1-P2-P3-P4-P5-P6 shown in Fig. 4a, from the buccal side to lingual side, are exhibited in Fig. 4c. The curves revealed the trend that stress at the cortical region is higher than that at cancellous region, at lingual side higher than at buccal side. For the new type of implant, wave crests of the curve correspond to cortical/cancellous boundary at both sides. At the lingual side, there is a rapid increase of stress in the boundary area and then the maximal stress was reached, subsequent to which was a steep decline. After coming to the lowest point, stress ascended gradually. The inclination is the same at buccal side, but the stress at the boundary is lower than cortical end. For traditional implant, stress distribution is closer to that of new implant at buccal side, but there is only an increase at lingual side. The stress of cortical bone along the path for traditional implant is higher than that for the new implant, especially at lingual side, with an increase of 39.7% at buccal side and 61.1% at lingual side. In the cancellous region, the new type of implant showed a relatively higher stress distributed than traditional implant.

3.2. Geometrical dimensional effects on the stress distribution of bone

To study the effects of varying the dimension of the new type of implant, mainly the depth and width of the gap between the inset and abutment, seven models with six kinds of depth size and two kinds of width size were investigated (Fig. 5).

In Fig. 5a, maximal stress of bone at the implant/bone interface for the seven models is drawn in column. Maximal stress in implants with zero gap depth is the highest, almost equal to traditional one. With the deepening of gap, maximal stress decreased. For implants of the adjacent size, significant declination is between the depth of 2 mm and 3 mm. Besides, the drop of maximal stress between gap depth of 7 mm and that of 9 mm is also prominent. On the other side, the difference between model d-9 and w-0.5, which differs only in gap width, is not so evident.

Stress distribution of bone at the implant/bone interface along the path P1-P2-P3-P4-P5-P6 (Fig. 4a) for the seven models has also been plotted, as shown in Fig. 5b. It can be drawn that the shape of curves for all models except model d-0 mm approximate, especially at the buccal side. Maximal stress ascended and situated approaching to the cortical end with the shortening of gap. Additionally, stress distribution of model d-0 mm resembles that of traditional implant to a large degree.

For implants, stress peak in implant for model d-0 mm, d-2 mm, d-3 mm, d-5 mm and d-7mm has little difference, which ranged from 670 MPa ~700 MPa. But a much higher stress peak, nearly 1200 MPa was observed in model d-9 mm and w-0.5 mm. This indicated gap depth that exceeded certain level would make implant unstable. Concluding, d-7 mm was more suitable for the design of new implant, with remarkably decreased bone stress and moderate implant stress peak.

3.3. Shape effects on stress distribution of bone

After choosing the suitable size of depth for implant, further investigation of abutment shape was given. It was observed from the contour plots of the bone with different shapes of new implant shown in Fig. 6a, b, c that of the implants in four shapes, tapered implant showed the highest maximal stress (MX) of 52.9 MPa, which was 9.5% higher than smooth cylindrical implant. Next in sequence was stepped implant, with maximal stress close to tapered one which was nearly 7.5% higher than smooth cylindrical one. Lowest maximal stress was obtained in screw implant (model s1). There was a marked decrease of 11.9 MPa for screw implant compared to

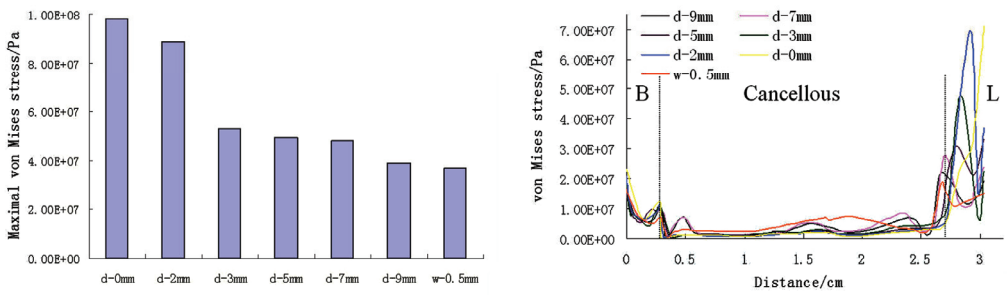

Fig. 5. Maximal stress of bone (left) at the implant/bone interface: left – maximal stress of bone for different types of implant model; right – path plots of bone stress for different implant model

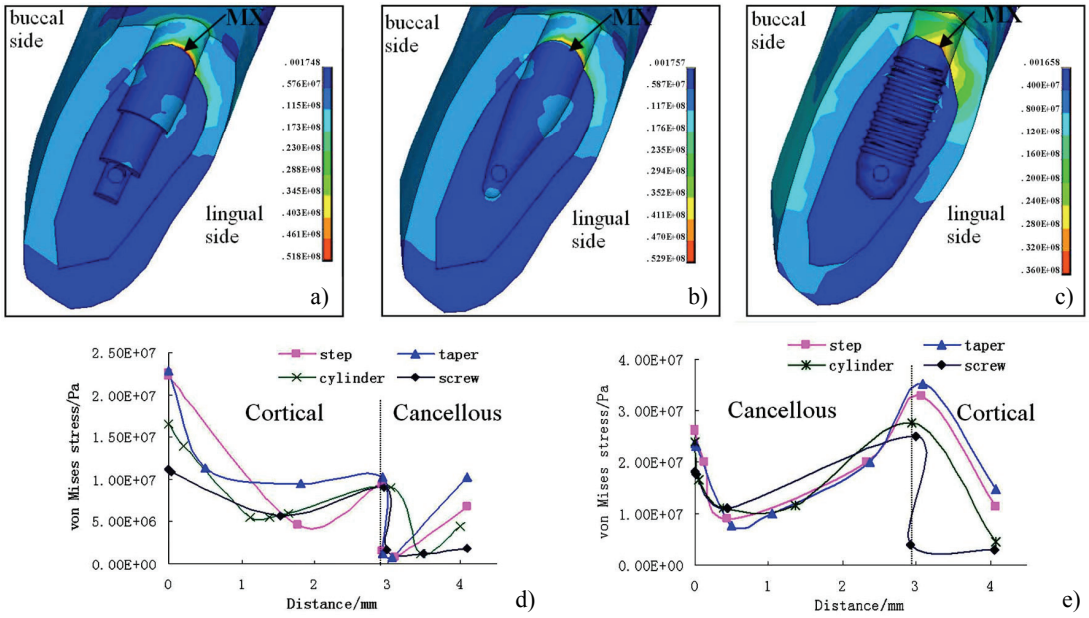

Fig. 6. Contour and path plots of interfacial stress of bone for model of different shapes:
a, b, c – contour plots of the bone with different shapes of new implant;
d, e – two paths from the top of cortical bone to the cancellous bone slightly below the cortical/cancellous boundary along the implant/bone interface

cylindrical one, nearly 24.8%. Stress peak created at the abutment for the four models is approximate.

Two paths from the top of cortical bone to the cancellous bone slightly below the cortical/cancellous boundary along the implant/bone interface were defined at the buccal side (P1-P2) and lingual side (P6-P5), respectively, as shown in Fig. 4a. Stress distribution along the two paths for implant of different shape is graphically represented in Fig. 6d, e. Obviously, screw implant exhibited a lower stress distribution compared to the other three implants, especially at the lingual side. Stress distribution of stepped and that of tapered implant were close, which were much higher than the other implants.

3.3. Variation in the screw length and pitch size for screw implant

Figure 7 shows contour plots of bone around screw implant model s2, s3 and s4. Comparison of the four screw implant models showed that maximal stress is lowest in model s1 (Fig. 6c) and model s2, which have little difference, while highest in model s4, above two folds of the former. For model s3, maximal stress of bone is about 39.5% higher than model s1 and model s2. The location of maximal stress lies in the cortical/cancellous boundary for all the screw implant models. The exact position is at the pitch end for model s3 and model s4.

There was no distinct deviation of the stress peak in both the value and location at the abutment for the four models.

4. Discussion

It was supposed that a gap between the inset and abutment plays the role of separating the two components major in the upper cortical layer, with the intention of conducting the force mostly to trabecular bone and thus reducing the stress peak induced in cervical cortex. In contrast to the original design, segment B of the inset in order to enhance the stability of the structure was added and its contacting area with the implant was sloped and edge filleted to make the force transferred more progressively. In the early studies, mandible model was simplified in FEA to test the design, which inevitably discounted the accuracy of results. Advanced CT and 3D reconstruction technology was employed in the study to reconstruct the precise jaw bone, providing a more favorable simulation environment [18]. On this basis, further investigation of this type of implant was applied. Results revealed a 51.6% reduction of the stress peak of this type of implants, compared to traditional one, demonstrating the viability of the design. Maximal stress located at the cortical/cancellous boundary for the new type of implant indicated that the force was passed from be-

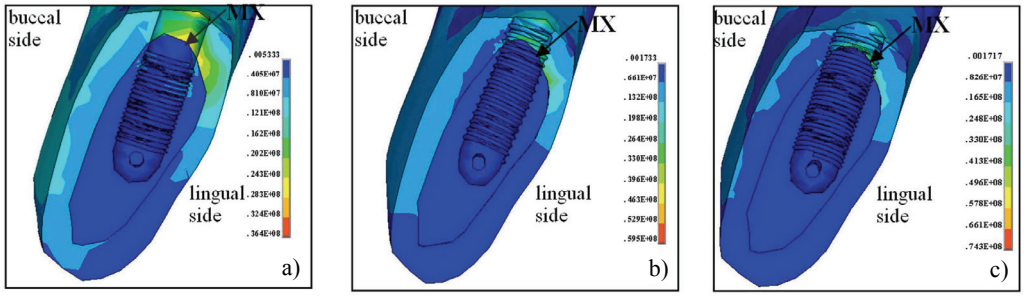

Fig. 7. Contour plots of von Mises stress distribution of bone with hidden implant for screw model s2, s3, s4 from cutaway view (a – model s2; b – model s3; c – model s4)

low, as described in previous study, avoiding the production of stress peak at the top of cortical layer by directly contacting with implant. Although there still existed a gain of stress at the top of cortical bone, but it remained a lower level. Change of stress distribution was remarkable at the lingual side, which was related closely to the direction of the load.

For the new type of implant, gap size was an effecting factor, confirmed by the results that with the increase of depth and width, stress peak of the surrounding bone presents an inclination of falling. Implant with no gap can be deemed as traditional implant. There is a sharp decline of stress from gap depth of 2 mm to that of 3 mm, and it can be explained that the force was still directly transferred to cortical bone for the former, as the cortical layer was about 3 mm thick. Another noticeable fall of stress is between the depth of 7 mm and 9 mm, revealing that the depth to some extent would lead to an obvious decrease of the stress peak. However, stress peak of the new type of implant exceeds that of the traditional one to a large degree, implying the larger potion of load taken by the inset. From this point, deepening and widening of the gap considerably would lead to the increase of instability of the implant. Therefore, picking appropriate gap size that can effectively decline the maximal stress of surrounding bone without the rising of stress peak at implant was of great importance for this new type of implant. Relative to gap depth, gap width exerted lesser impact on the stress distribution although the increment for width is much smaller as confined by design. The inclusive survey of the models with diverse gaze dimension revealed that gap depth of 7 mm and width of 0.3 mm would be applicable. Alternatively, large gap size could work if the inset can be designed to be easily removable and replaceable.

Results also revealed that among implants of the three shapes: cylindrical, tapered, stepped implant, cylindrical implant showed the lowest peak stress of surrounding bone. This may be in accordance with the result of Tsutsumi [19] and Siegele [20] that the most realistic shape for dental implant is cylinder. Petrie and Williams [21] also confirmed the superiority of cylinder implant to tapered one. Furthermore, introducing the screw to cylindrical implant embedded entirely in the cancellous bone would largely reduce the stress peak of bone which corroborates the previous studies [20, 22]. In this sense, screw plays the role of enlarging the contacting surface with bone which would reduce the stress of surrounding bone [19]. But as for this new type of implant, the screw functioned only applied in the cencellous region, beacause the extension to cortical region would conversely make the stress peak of bone promoted much higher. Details of the screw were also studied, showing that large pitch size would be preferable, which was in accordance with the findings of Chun et al. [23]. The results suggested that in condition of modicum amount of trabicular bone, large pitch size was advisable.

This work is of great significance not only in adopting the advanced model reconstruction technology in FEA to obtain reliable data to lend powerful reference and guidance to clinical application, but also in the design and optimization of the new type of implant which can extremely reduce the stress peak of cortical layer. The results would lend guidance to clinical application of dental implant.

References

[1] SUVA L.J., GADDY D., PERRIEN D.S., THOMAS R.L., FINDLAY D.M., *Regulation of bone mass by mechanical loading: microarchitecture and genetics*, Curr. Osteoporos. Rep., 2005, 3, 46–51.

[2] SCHOENAU E., *From mechanostat theory to development of the "Functional Muscle-Bone-Unit"*, J. Musculoskelet. Neuronal Interact., 2005, 5, 232–238.

[3] KUSZ D., WOJCIECHOWSKI P., CIELINSKI L.S., IWANIAK A., JURKOJC J., GASIOREK D., *Stress distribution around a TKR implant: are lab results consistent with observational studies?* Acta Bioeng. Biomech., 2008, 10, 21–26.

[4] SEVIMAY M., TURHAN F., KILICARSLAN M.A., ESKITASCIOGLU G., *Three-dimensional finite element analysis of the effect of different bone quality on stress distribution in an implant-supported crown*, J. Prosthet. Dent., 2005, 93, 227–234.

[5] DING X., ZHU X.H., LIAO S.H., ZHANG X.H., CHEN H., *Implant-bone interface stress distribution in immediately loaded implants of different diameters: a three-dimensional finite element analysis*, J. Prosthodont., 2009, 18, 393–402.

[6] HANSSON S., WERKE M., *The implant thread as a retention element in cortical bone: the effect of thread size and thread profile: a finite element study*, J. Biomech., 2003, 36, 1247–1258.

[7] MEIJER H.J., KUIPER J.H., STARMANS F.J., BOSMAN F., *Stress distribution around dental implants: influence of superstructure, length of implants, and height of mandible*, J. Prosthet. Dent., 1992, 68, 96–102.

[8] PIERRISNARD L., RENOUARD F., RENAULT P., BARQUINS M., *Influence of implant length and bicortical anchorage on implant stress distribution*, Clin. Implant Dent. Relat. Res., 2003, 5, 254–262.

[9] HIMMLOVÁ L., DOSTÁLOVÁ T., KÁCOVSKÝ A., KONVICKOVÁ S., *Influence of implant length and diameter on stress distribution: a finite element analysis*, J. Prosthet. Dent., 2004, 91, 20–25.

[10] BAGGI L., CAPPELLONI I., DI GIROLAMO M., MACERI F., VAIRO G., *The influence of implant diameter and length on stress distribution of osseointegrated implants related to crestal bone geometry: a three-dimensional finite element analysis*, J. Prosthet. Dent., 2008, 100, 422–431.

[11] SHIN Y.K., HAN C.H., HEO S.J., KIM S., CHUN H.J., *Radiographic evaluation of marginal bone level around implants with different neck designs after 1 year*, Int. J. Oral. Maxillofac. Implants, 2006, 21, 789–794.

[12] WANG X.J., WANG R.W., LUO J.Y., ZHANG X.D., *Preliminary evaluation of a new dental implant design with finite element analysis*, Key Eng. Biomater., 2005, 288–289, 657–660.

[13] RUBO J.H., SOUZA E.A., *Finite element analysis of stress in bone adjacent to dental implants*, J. Oral. Implantol., 2008, 34, 248–255.

[14] LIMBERT G., VAN LIERDE C., MURARU O.L., WALBOOMERS X.F., FRANK M., HANSSON S., MIDDLETON J., JAECQUES S., *Trabecular bone strains around a dental implant and associated micromotions–a micro-CT-based three-dimensional finite element study*, J. Biomech., 2010, 43, 1251–61.

[15] LIN D., LI Q., LI W., DUCKMANTON N., SWAIN M., *Mandibular bone remodeling induced by dental implant*, J. Biomech., 2010, 43, 287–293.

[16] IPLIKÇIOĞLU H., AKÇA K., *Comparative evaluation of the effect of diameter, length and number of implants supporting three-unit fixed partial prostheses on stress distribution in the bone*, J. Dent. 2002, 30, 41–46.

[17] CRAIG R.G., *Restorative Dental Materials*, ed. 6. St. Louis, CV Mosby Co., 1980.

[18] OZEN M., SAYMAN O., HAVITCIOGLU H., *Modeling and stress analyses of a normal foot-ankle and a prosthetic foot-ankle complex*, Acta Bioeng. Biomech., 2013, 15, 19–27.

[19] TSUTSUMI S., FUKUDA S., TANI Y., *Biomechanical designing of implants*, J. Dent. Res., 1989, 68, 766–774.

[20] SIEGELE D., SOLTESZ U., *Numerical investigations of the influence of implant shape on stress distribution in the jaw bone*, Int. J. Oral. Maxillofac. Implants, 1989, 4, 333–340.

[21] PETRIE C.S., WILLIAMS J.L., *Comparative evaluation of implant designs: influence of diameter, length, and taper on strains in the alveolar crest. A three-dimensional finite-element analysis*, Clin. Oral. Implants Res., 2005, 16, 486–494.

[22] TADA S., STEGAROIU R., KITAMURA E., MIYAKAWA O., KUSAKARI H., *Influence of implant design and bone quality on stress/strain distribution in bone around implants: a 3-dimensional finite element analysis*, Int. J. Oral. Maxillofac. Implants, 2003, 18, 357–368.

[23] CHUN H.J., CHEONG S.Y., HAN J.H. et al., *Evaluation of design parameters of osseointegrated dental implants using finite element analysis*, J. Oral. Rehabil., 2002, 29, 565–574.